Peptide Modified Electrospun Glycopolymer Fibers

Andrea Fiorani, Filbert Totsingan, Antonio Pollicino, Yifeng Peng, Maria Letizia Focarete, Richard A. Gross,* Mariastella Scandola*

Oligo(Glu_{70}-*co*-Leu_{30}), a peptide synthesized by protease catalysis, is functionalized at the N-terminus with a 4-pentenoyl unit and grafted to polyLSL[6′Ac,6″Ac], a glycopolymer prepared by ring-opening metathesis polymerization of lactonic sophorolipid diacetate. First, polyLSL[6'Ac,6"Ac] fiber mats are fabricated by electrospinning. Oxidation of the fiber mats and subsequent reaction with cysteamine lead to thiol-functionalized fiber mats with no significant morphology changes. Grafting of the alkene-modified oligopeptide to thiol-functionalized polyLSL[6′Ac,6″Ac] fiber mats is achieved via "thiol-ene" click reaction. X-ray photoelectron spectroscopy analysis to characterize peptide grafting reveals that about 50 mol% of polyLSL[6′Ac,6″Ac] repeat units at fiber surfaces are decorated with a peptide moiety, out of which about 1/3 of the oligo(Glu_{70}-*co*-Leu_{30}) units are physically adsorbed to polyLSL[6′Ac,6″Ac]. The results of this work pave the way to precise engineering of polyLSL fiber mats that can be decorated with a potentially wide range of molecules that tailor surface chemistry and biological properties.

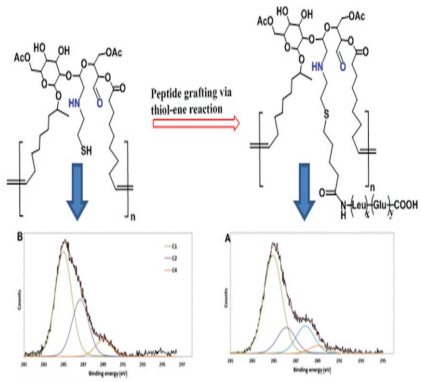

Dr. A. Fiorani, Prof. M. L. Focarete, Prof. M. Scandola
Department of Chemistry 'G. Ciamician'
University of Bologna
Via Selmi 2, 40126 Bologna, Italy
E-mail: mariastella.scandola@unibo.it
Dr. F. Totsingan, Dr. Y. Peng, Prof. R. A. Gross
Department of Chemistry and Chemical Biology
Center for Biotechnology and Interdisciplinary Studies
Rensselaer Polytechnic Institute
110 8TH ST, Troy, NY 12180, USA
E-mail: grossr@rpi.edu
Prof. A. Pollicino
Department of Industrial Engineering
University of Catania
95125 Catania, Italy
Dr. Y. Peng
Department of Chemical and Biomolecular Engineering
NYU Polytechnic School of Engineering
Sixth Metrotech Center
Brooklyn, NY 11201, USA

1. Introduction

Bioresorbable materials bearing functionalities that enable the introduction of biologically active molecules are critically important for a wide range of applications including drug delivery, tissue engineering, and bioadhesives.[1–4] Natural polymers such as polysaccharides and proteins are important families of functional bioresorbable materials that offer potential advantages such as biological recognition. Notable examples include hyaluronic acid, a glycosaminoglycan found in extracellular matrices,[5] pullulan, an extracellular water-soluble film-forming microbial polysaccharide that is biocompatible[6] and chitosan, a natural, cationic, and biodegradable polymer derived by chitin deacetylation.[7] However, drawbacks often associated with natural polymers include difficulties in purification, selective modification, poor thermal stability, and contamination. That is, for biomedical materials, the poor thermal stability of natural

Macromol. Biosci. **2016**, DOI: 10.1002/mabi.201600327

polymers prohibits their fabrication by conventional melt extrusion and injection molding.[8]

Synthetic polymers from purified monomers such as lactide, glycolide, ε-caprolactone, and lactonic sophorolipids overcome difficulties in thermal processing and concerns over contamination with impurities. A common strategy in synthesizing functional bioresorbable polymers is to design copolymers consisting of either glycolide (GA), lactide (LA), ε-caprolactone (ε-CL), 1,5-dioxepan-2-one (DXO), or trimethyl carbonate (TMC) with a functionalized derivative of GA, LA, ε-CL, DXO, or TMC. A number of examples are given in reviews and other publications.[9–16] While these approaches have merit and may lead to important bioresorbable functional materials, they often involve tedious, chemically intensive methods that are not practical for scale-up and commercialization. Furthermore, copolymerization of protected functional monomers and deprotection chemistries often result in low copolymer molecular weights and corresponding poor biomaterial physical properties.

Guided by the rapid growth of knowledge of carbohydrate functions in biological contexts,[17,18] biomaterial scientists are exploring synthetic strategies to build carbohydrates into non-natural polymer constructs (e.g., synthetic glycopolymers) as pendant or terminal groups.[17,18] Indeed, glycopolymers hold promise for use in a broad range of biomedical applications. Generally, chemical routes to carbohydrate-decorated polymers with C—C main chains require chemically intensive synthetic approaches with protection–deprotection steps. Furthermore, with few exceptions, the backbones of synthetic glycopolymers are nondegradable.[19,20] The availability of glycopolymers that can degrade in biological environments would be beneficial for many in vivo biomaterial applications.[21]

Sophorolipids (SLs) are a member of a family of microbially produced glycolipids, which are produced in large quantities by *Candida bombicola*.[22–24] Previous work has addressed the potential conversion of SLs into unique glycopolymers. In the first attempt by our research team, SLs were appended to acrylate monomers by a multistep synthetic approach resulting in non-degradable C—C main chains.[25] In addition, Hu and Ju reported the lipase-catalyzed ring-opening polymerization (ROP) of lactonic SLs, which provided low molar mass polymers.[26] Subsequently, our research team, in collaboration with Coughlin, found that ring-opening metathesis polymerization (ROMP) of lactonic sophorolipid diacetate, LSL[6′Ac,6″Ac] affords an efficient route to transfer the imbedded complexity within natural SLs to high molecular weight (M_n up to 103 000 g mol^{-1}) poly(sophorolipid), polyLSL[6′Ac,6″Ac] (Figure 1).[27] This unique member of the synthetic glycopolymer family consists of alternating hydrophobic and hydrophilic segments reflecting its amphiphilic structure.[27–29] Since the chain has glycosidic and ester links, polysophorolipids are fully bioresorbable. Furthermore, primary hydroxyl functional groups along chains provide reactive moieties that can be selectively modified to tune polyLSL physical properties.[30] Recently, we reported that polyLSLs are cytocompatible with human mesenchymal stem cells (h-MSCs) and that changes in lactonic sophorolipid (LSL) functionality have the potential to modulate h-MSC lineage progression.[31] Furthermore, we showed that variation of substitution at sophorose 6′ and 6″ sites that occur repetitively along polyLSL chains remarkably influence material thermal properties, degradation rate, and osteogenic response.[31] In addition, synthetic routes were developed for functionalization of polyLSLs with clickable methacrylate and azide functional groups to facilitate attachment of bioactive moieties.[31]

Continuous nanofibers produced through electrospinning can be assembled into highly porous (typically

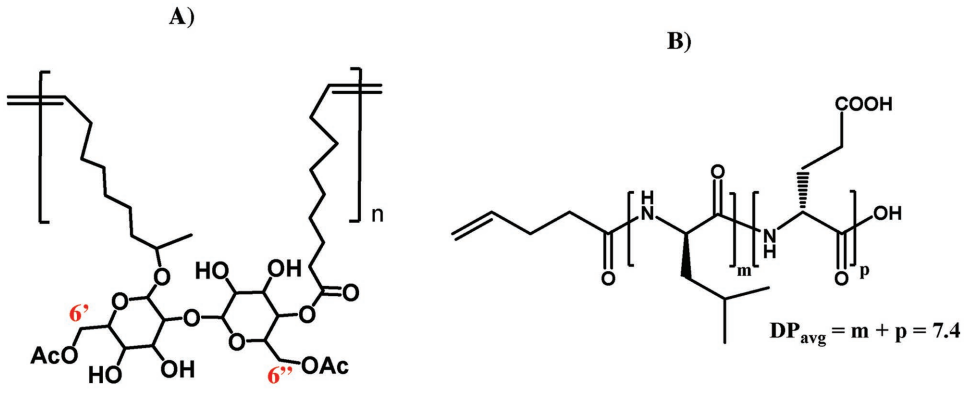

Figure 1. Chemical structures of: A) diacetylated poly(lactonic sophorolipid), polyLSL[6′Ac,6″Ac] and B) N-(4-pentenoyl) modified oligo(Glu_{70}-*co*-Leu_{30}).

Macromol. Biosci. **2016**, DOI: 10.1002/mabi.201600327

above 80%) matrices with remarkable specific area and interconnectivity of both pores and fibers. These unique properties have led to the use of electrospun constructs in diverse fields such as tissue engineering and drug delivery.[32,33] Many synthetic and natural polymers have been successfully electrospun to produce scaffolds with controlled fiber alignment to direct cell adhesion, orientation, and proliferation. The incorporation of biologically active molecules into electrospun fibers enables the engineering of scaffold matrices for the delivery of growth factors, enzymes, drugs, etc.[34] A parallel topic is electrospun fiber surface functionalization by physical or chemical approaches. The ability to introduce various chemical functionalities and bioactive moieties on electrospun fibers allows for the tuning of corresponding matrices so they can display desired chemical and biological features.[35]

The solid state properties of polyLSL[6′Ac,6″Ac] were reported in a previous study by this research team.[29] In summary, the polymer is a solid at room temperature which undergoes a glass transition at 61 °C and has a crystal phase that melts at 123 °C. The crystal phase consists of ordered packing of aliphatic chain segments and long-range order of sophorose groups.

In this work, we report fabrication and solid-state characterization of polyLSL[6′Ac,6″Ac] electrospun fibers. Furthermore, a versatile method is described by which peptides were conjugated to sophorose moieties of polyLSL[6′Ac,6″Ac] non-woven mats. X-ray photoelectron spectroscopy (XPS) was used to monitor surface modification reactions. The modification of the glycopolymer fiber mat with a model peptide was performed in order to establish an effective strategy by which bioactive peptides, proteins, or ligands of cell surface receptors can be covalently bound to the surface of this unique bioresorbable and biocompatible polymeric material. The primary hydroxyl functional groups along chains of polyLSL are exploited as reactive moieties for the peptide conjugation reaction steps. The results of this work pave the way for precise engineering of polyLSL fiber mats that can be decorated with a potentially wide range of molecules that tailor surface chemistry and biological properties.

2. Experimental Section

2.1. Materials

Lactonic sophorolipid acetylated at the 6′ and 6″ sophorose ring positions, LSL[6′Ac,6″Ac], was produced by fermentation of *Candida bombicola* following a previously published protocol.[24,36] L-Glutamic acid diethyl ester hydrochloride (L-Glu(OEt)$_2$·HCl) and L-leucine ethyl ester hydrochloride (L-Leu-OEt·HCl) were purchased from Tokyo Kasei Co. Ltd. Crude papain (cysteine protease; EC 3.4.22.2; source, *Carica papaya*; 30 000 USP units per mg of solid; molecular weight 21 K) was purchased from CalBioChem. Co. Ltd. Tetrahydrofuran (THF), N,N-dimethylformamide (DMF), sodium periodate, sodium cyanoborohydride, and cysteamine (CA) were purchased from Sigma-Aldrich. All chemicals and solvents were purchased in the highest available purity and were used without further purification.

2.2. Synthesis of N-(4-pentenoyl)oligo(Glu$_{70}$-*co*-Leu$_{30}$)

Oligo(γ-EtGlu$_{70}$-*co*-Leu$_{30}$-OEt) was prepared by protease-catalyzed oligopeptide synthesis.[37] Briefly, a mixture of L-Glu(OEt)$_2$·HCl (1.75 mmol), L-Leu-OEt·HCl (0.75 mmol), papain (16 units per mL) and 5 mL phosphate buffer solution (pH 8.0, 0.9 M) was reacted with stirring for 4 h at 40 °C. After cooling to room temperature, the peptide precipitate was collected by centrifugation (6000 rpm), washed and lyophilized giving a white powder (yield: 68%; DP_{avg}: 7.4). The yield was determined gravimetrically and the DP_{avg} was measured by ^{1}H-NMR end-group analysis as is described elsewhere.[37]

The N-terminus of the peptide (258 mg) was modified by reaction with 4-pentenoyl chloride (2eq) in DMF (5 mL) using triethylamine (2eq) as base. The reaction mixture was stirred at room temperature for 18 h and the modified peptide was precipitated by addition of cold water. The white precipitate was collected, washed three times with cold water, and lyophilized (yield: 77%). To remove pendant ethyl ester moieties, the lyophilized powder (156 mg) was suspended in 2 N NaOH solution (10 mL) at 60 °C and stirred for 30 h. The solution was then acidified to pH 4.0, dialyzed to remove salts (MWCO = 100–500 Da) and lyophilized to yield the desired product, which was confirmed by ^{1}H NMR.

2.3. Synthesis of Diacetylated Poly(sophorolipid), PolyLSL[6′Ac,6″Ac]

The ROMP of LSL[6′Ac,6″Ac] was performed following a previously published method.[28,31] Briefly, the polymerization of LSL[6′Ac,6″Ac] was conducted in anhydrous tetrahydrofuran for 30 min at 60 °C using the Grubbs second generation (G2) catalyst. The polymer was purified by dissolution in THF and subsequent precipitation in ethanol. The number average molecular weight (M_n) and dispersity ($Đ$, M_w/M_n) of the obtained polymer were determined by Gel Permeation Chromatography (GPC).

2.4. Electrospinning of p(SL) Fibers

Electrospinning was performed using a homemade apparatus. Briefly, polyLSL[6′Ac,6″Ac] was dissolved in THF/DMF (90/10, v/v) at a concentration of 16% by weight. A glass syringe containing the polyLSL[6′Ac,6″Ac] solution was connected to a stainless-steel blunt-ended needle through a Teflon tube. The needle (inner diameter 0.84 mm) was connected to a high voltage power supply (Spellman SL 50 P 10/CE/230) and a grounded aluminum plate was used as the collector. The needle-to-collector distance was fixed at 20 cm and the potential was 20 kV. The polyLSL[6′Ac,6″Ac] solution feed rate, controlled by a syringe pump (KD Scientific 200 series), was 0.9 mL h^{-1}. During

electrospinning, the temperature and relative humidity were kept constant at 25 °C and 48%, respectively.

2.5. Surface Chemical Functionalization of PolyLSL[6′Ac,6″Ac] Fiber Mats

In order to covalently graft the oligo(Glu_{70}-*co*-Leu_{30}) at the fiber surface, the synthesis was carried out according to the following steps.[38–41] First, oxidation of polyLSL[6′Ac,6″Ac] mats at 2,3-diol moieties of sophorose units was performed by adapting literature methods.[39] Briefly, periodate was used as the oxidant to convert 2,3-diols to dialdehyde groups. The mats (10 mg) were cut and fixed on polycarbonate rings (Scaffdex cell crown 24), which were immersed in 10 mL of phosphate-buffered saline (PBS) 0.1 M (pH 4.5) and $NaIO_4$ (10 mg mL^{-1}) for 2 h at 30 °C in a shaker-incubator. The molar ratio of polyLSL[6′Ac,6″Ac] repeating unit and periodate is about 1 to 3. Oxidized polyLSL[6′Ac,6″Ac] mats were rinsed in distilled water three times and dried. Reductive amination with CA was then performed by adapting a literature method[40] to introduce free thiol groups. Briefly, oxidized mats (10 mg) were reacted with CA (22 mg) and sodium cyanoborohydride (18 mg) in 10 mL of 0.1 M PBS (pH 7.5) for 2 h at 30 °C in a shaker-incubator. The molar ratio of oxidized polyLSL[6′Ac,6″Ac] repeating unit and CA/sodium cyanoborohydride is about 1:20. Aminated mats were rinsed in distilled water three times and dried. To determine whether CA physical adsorption occurs, non-oxidized mats were incubated with CA and sodium cyanoborohydride and rinsed with distilled water as above. Subsequently, the washed mats were analyzed by XPS as described below to determine the extent of CA physical adsorption. For thiol functionalized mats, thiol-ene conjugation of terminal alkene functionalized peptides was performed by adapting a literature method.[41] Briefly, N-(4-pentenoyl)oligo(Glu_{70}-*co*-Leu_{30}) (13 mg) was dissolved in 4 mL double-distilled water and thiol functionalized mats (10 mg) were added. Then 0.3 mol% of the radical photoinitiator 2,2-dimethoxy-2-phenyl acetophenone (DMPA) was added to the oligopeptide. The solution was UV irradiated at 365 nm for 1 h at room temperature with magnetic stirring. Oligo(Glu_{70}-*co*-Leu_{30}) functionalized mats were rinsed in distilled water three times and dried. As a control to assess the extent to which oligopeptide may be physically adsorbed to mats, thiol functionalized mats were reacted with N-(4-pentenoyl)oligo(Glu_{70}-*co*-Leu_{30}) exactly as was described above except without UV radiation.

2.6. Compression Molding of Films

Films were obtained by hot pressing polyLSL[6′Ac,6″Ac] between Teflon sheets in a Carver press at 150 °C for 1 min. The obtained films (0.2 mm thick) were cooled to room temperature in the press by using the built-in cooling circuit.

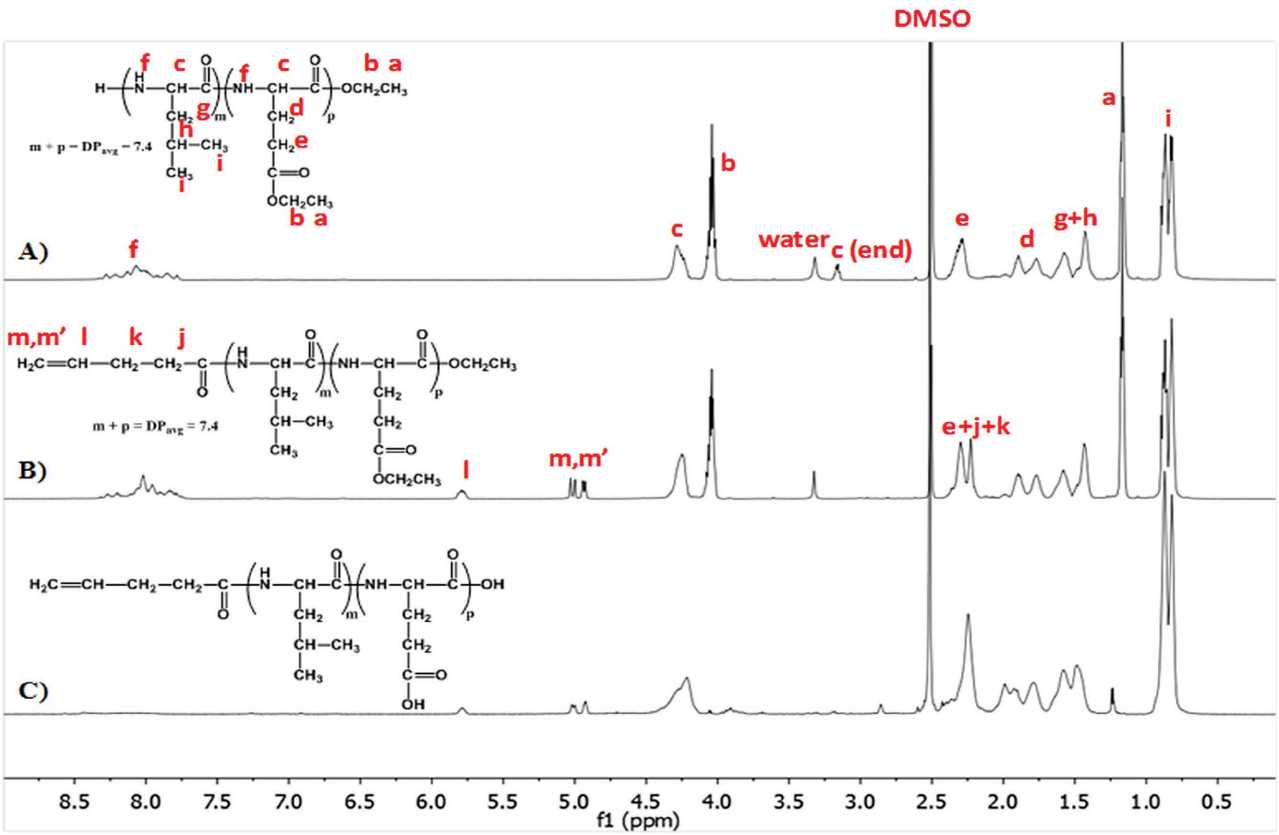

Figure 2. ^1H NMR (600 MHz) spectra in DMSO-d_6 of A) oligo(γ-EtGlu$_{70}$-*co*-Leu$_{30}$-OEt), B) N-(4-pentenoyl)oligo(γ-EtGlu$_{70}$-*co*-Leu$_{30}$-OEt), and C) the corresponding hydrolyzed alkene-linked peptide in DMSO-d_6/TFA-d (10:1).

Macromol. Biosci. **2016**, DOI: 10.1002/mabi.201600327

2.7. Characterization Methods

2.7.1. Scanning Electron Microscope (SEM)

Fiber morphology was imaged using a Philips 515 SEM at an accelerating voltage of 15 kV. Samples were sputter-coated with gold prior to imaging. The average fiber diameter was determined by measuring about 250 fibers using image acquisition and analysis software (EDAX Genesis).

2.7.2. Tensile stress–strain Measurements

Analyses of both films and electrospun mats were performed at room temperature using an Instron Testing Machine 4465 (cross-head speed 2 mm min^{-1}). Nine rectangular specimens (width = 5 mm, gauge length = 20 mm) were analyzed for each sample. The specimen thickness, measured with a digital micrometer, was used to obtain stress–strain curves from raw load–displacement data. Stress and strain at yield (σ_y and ε_y), stress and strain at break (σ_b and ε_b) as well as the tensile modulus (E) were determined as the average value ± standard deviation.

2.7.3. Thermogravimetric Analysis (TGA)

Measurements were performed using a TA Instruments TGA2950 thermogravimetric analyzer at 10 °C min^{-1} from room temperature to 600 °C, both under nitrogen and under air purge.

2.7.4. Differential Scanning Calorimetry (DSC)

Measurements were performed using a TA Instruments Q100 DSC equipped with the LNCS low-temperature accessory. Thermal scans were performed from −80 to 200 °C, at a heating rate of 20 °C min^{-1}, in a helium atmosphere. Quench cooling was applied between heating scans. The glass transition temperature (T_g) was taken at the midpoint of the stepwise specific heat increment, while the melting temperature (T_m) was taken at the maximum of the endothermal peak.

2.7.5. XPS

Surface chemical composition of as-synthesized and modified polyLSL[6′Ac,6″Ac] fiber mats was determined by XPS using a VG Instrument electron spectrometer using a Mg $K_{\alpha 1,2}$ X-ray source (1253.6 eV). The X-ray source under standard conditions was at 300 W, 15 kV, and 20 mA. The base pressure of the instrument

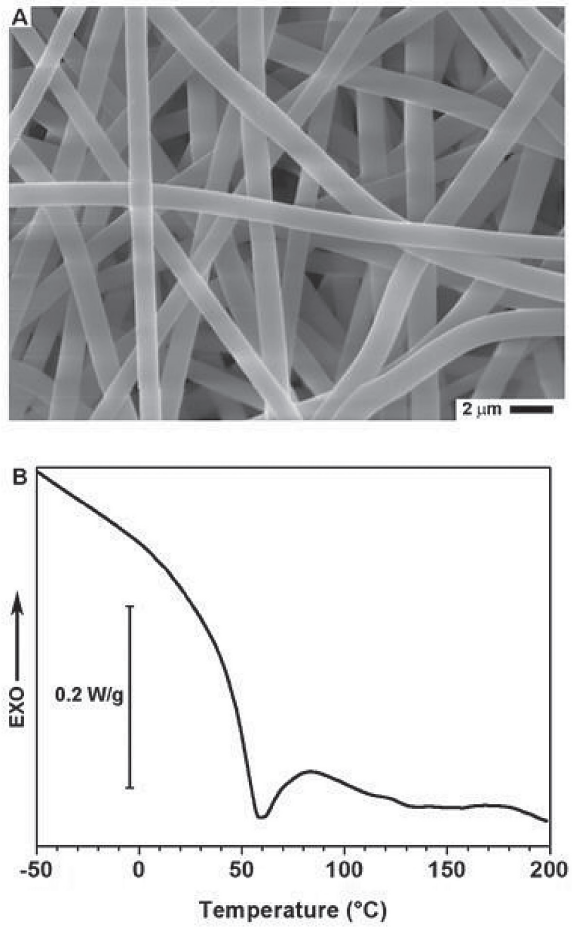

Figure 3. Electrospun polyLSL[6′Ac,6″Ac] fiber mat: A) SEM micrograph and B) first heating scan DSC curve.

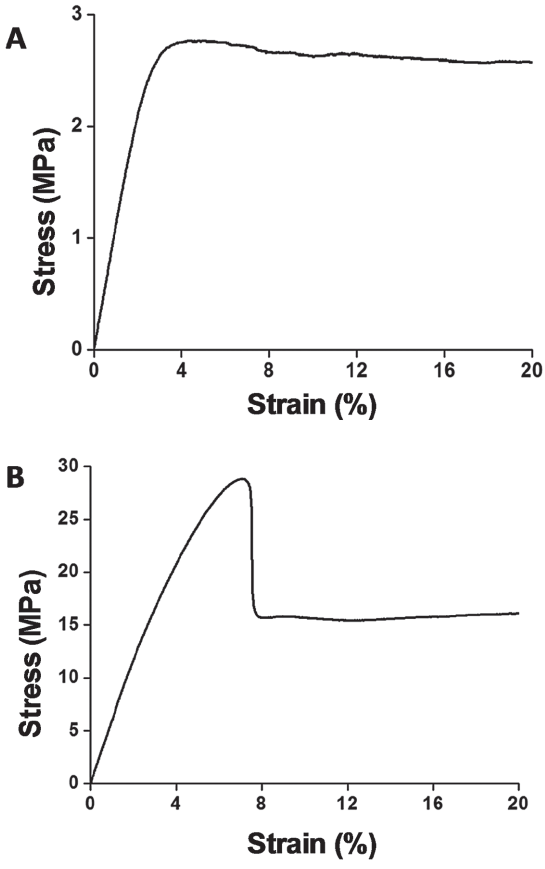

Figure 4. Stress–strain curves of polyLSL[6′Ac,6″Ac] in the form of: A) An electrospun mat, B) compression molded film. Curves are reported up to 20% strain.

Macromol. Biosci. **2016**, DOI: 10.1002/mabi.201600327

Table 1. Mechanical properties of polyLSL[6′Ac,6″Ac] film and electrospun mat: stress at yield (σ_y), strain at yield (ε_y), elastic modulus (E), strain at break (ε_b). Average values with standard deviations are reported.

PolyLSL[6′Ac,6″Ac] processed form	σ_y [MPa]	ε_y [%]	E [MPa]	ε_b [%]
Film	27.7 ± 3.8	7 ± 2	681 ± 136	>200
Fiber mat	2.7 ± 0.1	5 ± 1	112 ± 6	206 ± 22

was 5×10^{-10} Torr and an operating pressure of 2×10^{-8} Torr was adopted. Widescan acquisitions were carried out using a pass energy of 100 eV, while narrowscans were acquired using a pass energy of 20 eV. Semi-quantitative surface analyses were performed by determining photoelectron peak areas obtained by multiplying the experimental values with the appropriate sensitivity factor. Spectral acquisition take-off angles (t.o.a) of 45° and 80° were used. Considering that the relationship between the sampling depth (d) and the t.o.a (θ) is represented by the equation $d = 3\lambda \sin\theta$, where λ is the inelastic mean free path of the photoelectrons (for carbon $\lambda = 14$ Å),[42] the thickness of analyzed layers is about 30 and 40 Å for t.o.a of 45° and 80°, respectively. The calculation of the areas corresponding to the different photoelectron peaks was performed using VGX900x software; the curve fitting elaborations were determined by PeakFit software (version 4, from SPSS Inc.). The curve fitting of the C_{1s} envelope was determined as the product of Gaussian and Lorentzian functions (80:20): the full width at half maximum of each curve was kept equal to 1.7 ± 0.1 eV. Binding energies referred to the C—H level at 285 eV.

3. Results and Discussion

3.1. Oligopeptide Structure Analysis

Oligo(γ-Et-L-Glu$_{70}$-*co*-L-Leu$_{30}$), synthesized by papain-catalysis (40 °C, 4 h, feed ratio = 70:30), was obtained having a DP_{avg} = 7.4 (from ^{1}H NMR, Figure 2A) in 68% yield. These results are consistent with previously reported values on peptides of the same composition.[37] Alkene-functionalization at the N-terminus was achieved in 77% yield by reaction of oligo(γ-Et-L-Glu$_{70}$-*co*-L-Leu$_{30}$) with 4-pentenoyl chloride. The ^{1}H NMR spectrum in deuterated dimethyl sulfoxide (DMSO-d$_6$), along with peak positions and assignments, is displayed in Figure 2B. The new signals appearing at 4.9–5.8 ppm are typical of alkenylic protons and were assigned to protons **l, m,** and **m′** of the 4-pentenoyl unit. To remove the C-terminal and pendant ethyl ester residues, hydrolysis was performed using 2N NaOH. The ^{1}H NMR

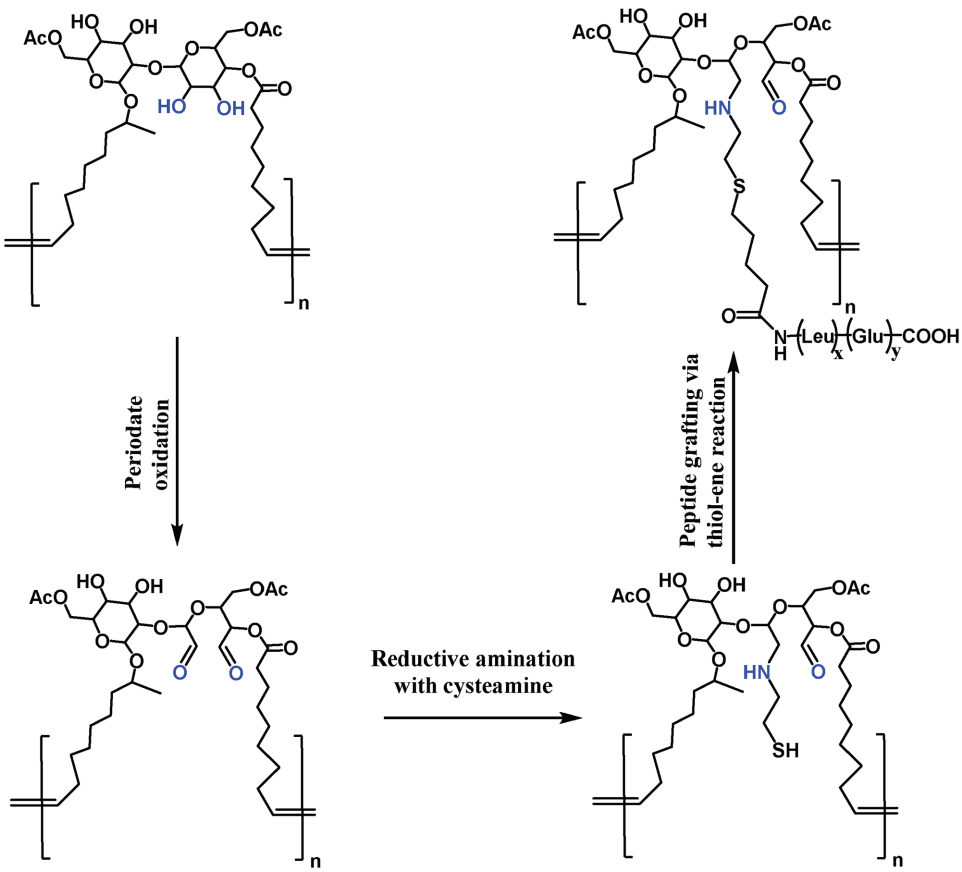

Scheme 1. Route to graft peptides to polyLSL[6′Ac,6″Ac].

Macromol. Biosci. 2016, DOI: 10.1002/mabi.201600327

spectrum in deuterated dimethyl sulfoxide (DMSO-d_6)-Trifluoroacetic acid (TFA-d) mixture (10:1) of the hydrolyzed peptide is reported in Figure 2C. The two signals at 1.17 ppm and 4.05 ppm, which were assigned to a) methyl and b) methylene protons of ethyl ester moiety, respectively, completely disappeared upon hydrolysis.

3.2. Fabrication of PolyLSL[6′Ac,6″Ac] Fiber Mats

Electrospinning of polyLSL[6′Ac,6″Ac] was performed under optimized conditions reported in the Experimental Section. By this method, beadless, good morphology fibers that are circular in shape and randomly orientated were obtained (Figure 3). Measured fiber diameters are 1.19 ± 0.16 μm. DSC and TGA analyses of polyLSL[6′Ac,6″Ac] non-woven mats prepared by electrospinning were performed. TGA analysis does not show differences compared to the earlier reported TGA results on polyLSL[6′Ac,6″Ac] powder.[29] Furthermore, the TGA thermogram indicates the absence of residual solvent in electrospun fibers. The only thermal event in the DSC curve (first scan, Figure 3) is the glass transition showing that, during electrospinning, the solvent undergoes very fast evaporation that does not allow polymer crystallization.

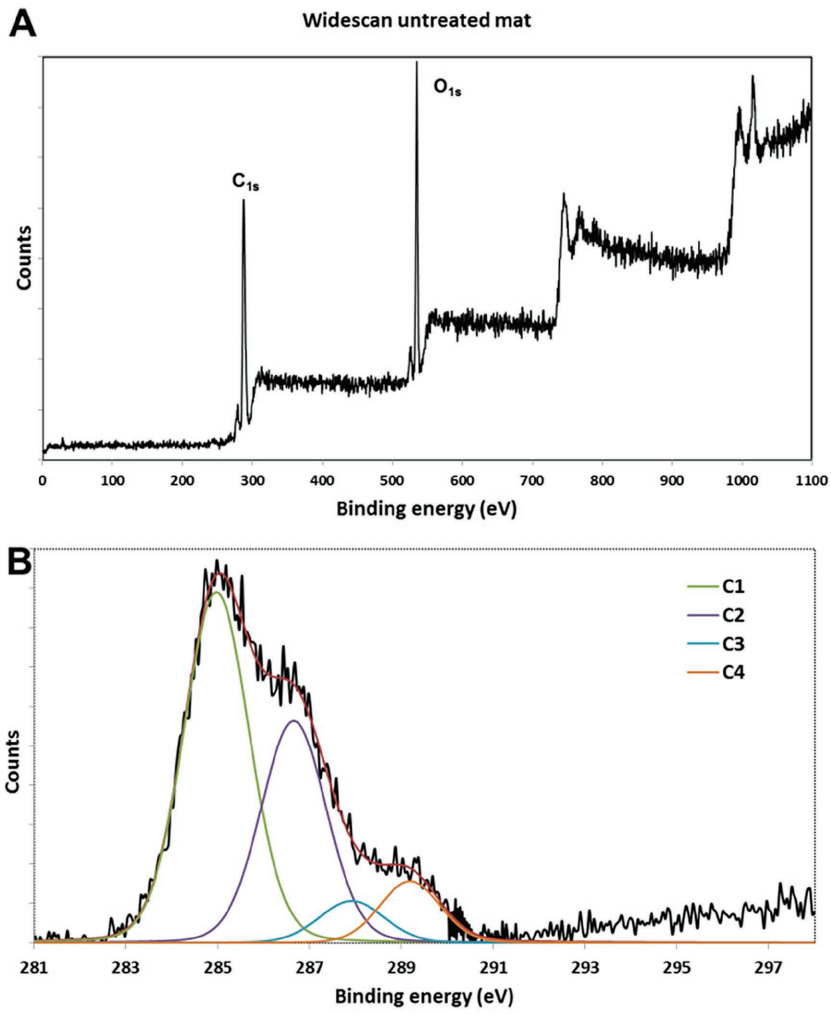

Figure 5. Untreated polyLSL[6′Ac,6″Ac] mat XPS spectra (t.o.a 45°): A) Widescan, B) C_{1s} envelope and its components.

Tensile stress–strain measurements were run for polyLSL[6′Ac,6″Ac] electrospun fiber mats. For comparison, Figure 4 displays representative stress–strain curves for the fiber mat and compression molded polyLSL[6′Ac,6″Ac] film. The corresponding mechanical property data are collected in Table 1. The elastic modulus and strength at yield of the fiber mat are much lower than that for polyLSL[6′Ac,6″Ac] film. This result is consistent with fiber mat high porosity, the unavoidable overestimation of fiber mat specimen cross sectional area and that the orientation of fibers within mats are random. The elastic modulus and strength at yield of mats will begin to approach that of films if they are formed with isoaligned fibers.[43]

3.3. Surface Functionalization of Electrospun PolyLSL[6′Ac,6″Ac] Mats

The reactions carried out in order to ″graft″ oligo(Glu_{70}-*co*-Leu_{30}) to fiber surfaces were conducted as described in the Experimental Section. Briefly, the first reaction was an oxidation of the sophorose 2,3-diols to aldehydes using periodate, followed by a reductive amination using cysteamine to functionalize the fibers with thiol groups. Subsequently, the terminal alkene functionalized peptide was conjugated to the fibers by a thiol-ene reaction (Scheme 1).

In order to assess the success of polyLSL[6′Ac,6″Ac] functionalization reactions and, ultimately, peptide

Table 2. Relative abundance from C_{1s} envelope deconvolution of untreated and oxidized polyLSL[6′Ac,6″Ac] mats (t.o.a. 45°).

Sample		C1	C2	C3	C4
Untreated [%]	experimental	52	33	6	9
	calculated	53	32	6	9
Oxidized [%]		52	28	9	10

grafting, characterizations were performed by XPS at t.o.a of 45° and 80°. First, XPS analysis of native or non-modified polyLSL[6′Ac,6″Ac] mat was conducted (Figure 5A,B). From the repeat unit structure of polyLSL[6′Ac,6″Ac], and considering that hydrogen is not detected by XPS, the expected (theoretical) atomic abundances of carbon and oxygen were calculated. Assuming polyLSL[6′Ac,6″Ac] lacks hydrogen atoms, its repeat unit formula is $C_{34}O_{14}$. From this formula, the expected atomic ratio of O/C is 0.41. The XPS experimentally determined O/C ratio (Figure 5A) is 0.39, close to the expected value. The slightly higher carbon content may be due to the presence of hydrocarbon contamination that is often observed in XPS analysis of polymeric systems.[44] More information confirming the structure of the substrate surface is derived from analysis of the C_{1s} peak envelope (Figure 5B), i.e., from the relative abundance of carbons that differ in attached atoms. From the structure of the repeat unit, four chemical states can be identified and their position and relative abundance predicted: C1 (285 eV) that is due to the 16 carbons of the ω-1-hydroxyl C18 moiety and to the 2 carbons of the Ac groups that are linked to other carbon or hydrogen atoms (C—C or C—H); C2 (286.6 eV) due to the 11 carbon atoms linked by a single bond to an oxygen atom (C—O); C3 (287.9 eV), due to the two carbon atoms linked via a single bond to two oxygen atoms O—C—O; C4 (289.2 eV), due to the 3 carbon atoms that comprise carbonyl moieties of carboxylate ester groups (O—C=O). Hence, the peak fitting elaboration of the C_{1s} envelope (Figure 5B) perfectly matches predictions both in terms of peak position and relative abundance (Table 2), confirming the polymer structure. The polymer mats were subjected to the various synthetic steps and the changes in XPS curves were analyzed.

The results of XPS analysis after the oxidation reaction with periodate are reported in Figure 6. From peak-fitting

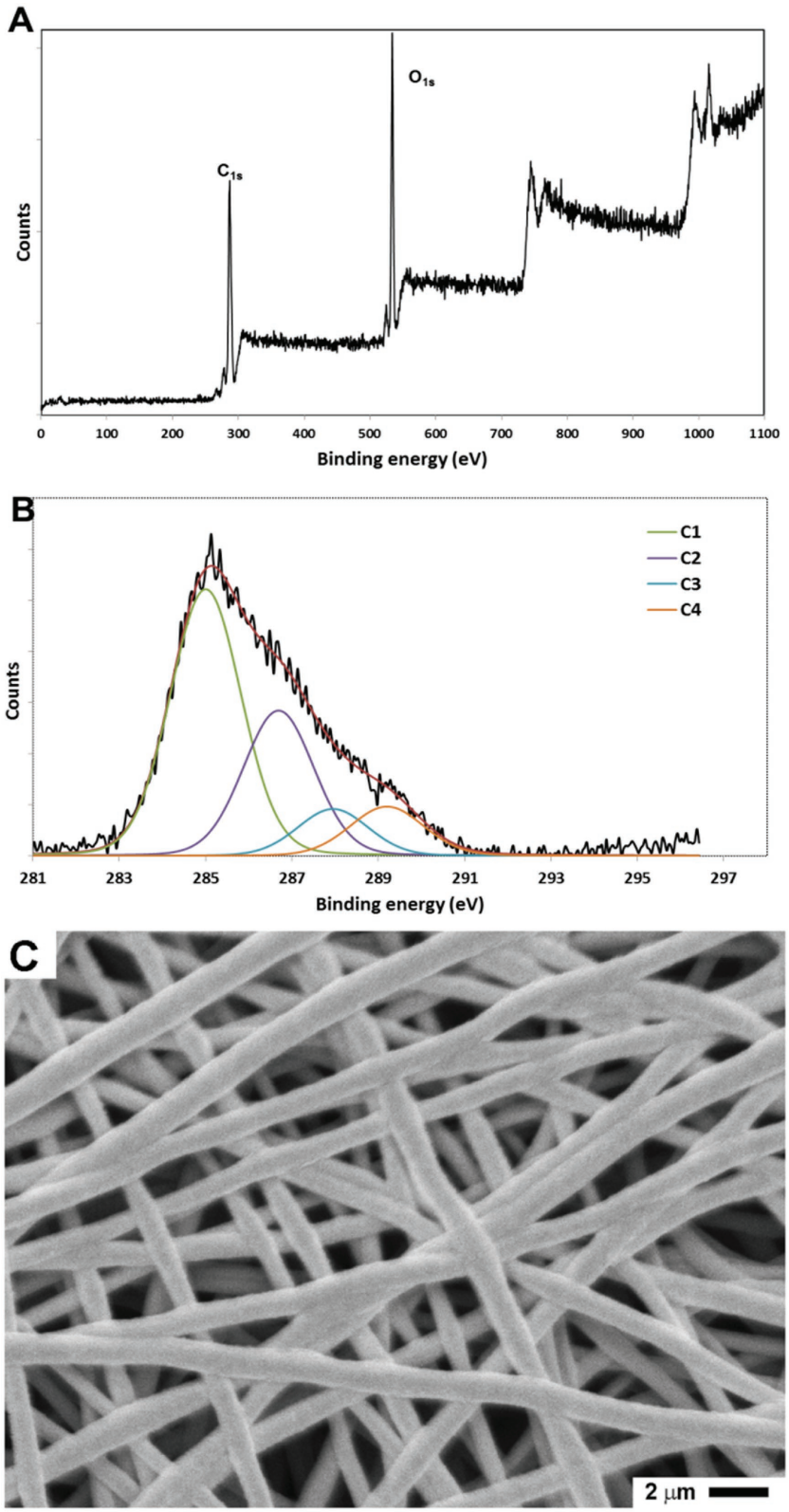

Figure 6. Oxidized polyLSL[6′Ac,6″Ac] mat: A) XPS spectra (t.o.a 45°) widescan, B) C_{1s} envelope and its components, C) SEM micrograph.

Macromolecular Journals

Macromol. Biosci. **2016**, DOI: 10.1002/mabi.201600327

analysis, the relative abundance of C_{1s} envelope constituents of untreated and oxidized polyLSL[6′Ac,6″Ac] mats (t.o.a. 45°) was obtained and is listed in Table 2. The C2 component decreases (i.e., carbon atoms singly bonded to oxygen), while the C3 peak intensity increases (carbon atoms doubly bonded to oxygen), consistent with the conversion of 2,3-diol moieties to dialdehydes. The conversion of 2,3-diol alcohols to dialdehydes reaches almost 25% in the surface layer tested by XPS at t.o.a. 45° (expected values of C_{1s} deconvolution in this hypothesis: C1 = 53%, C2 = 29%, C3 = 9% and C4 = 9%). In other words, considering two repeating units, of the eight hydroxyl groups of which half are 2,3-diols susceptible to diol oxidation, on average one 2,3-diol is converted to a dialdehyde moiety.

SEM analysis of polyLSL[6′Ac,6″Ac] mat fiber morphology after periodate oxidation showed only minor, not significant, changes (Figure 6C). Subsequently, reductive amination of dialdehydes was performed with cysteamine and sodium cyanoborohydride (Scheme 1). This step enables the covalent attachment of amines by formation of a C—N bond and, consequently, the introduction of thiol moieties. The results of XPS analysis on the aminated fiber mats are shown in Figure 7A,B and the relevant atomic ratios are collected in Table 3.

In order to determine the average number of aldehyde groups that reacted with an amine, theoretical relationships were developed that correlate the extent of modification and corresponding atomic ratios (O/C, N/C, N/O) that would result. The equations given below describe these correlations

For O/C ratio

$$n^\circ \textit{ of cysteamine} = 30.552(O/C)^2 - 42.681(O/C) + 12.429 \quad (1)$$

For N/C ratio

$$n^\circ \textit{ of cysteamine} = 101.59(N/C)^2 + 31.95(N/C) + 0.0348 \quad (2)$$

For N/O ratio

$$n^\circ \textit{ of cysteamine} = -7.5367(N/O)^2 + 12.866(N/O) + 0.0577 \quad (3)$$

where n° is the number of cysteamine units conjugated to each polyLSL[6′Ac,6″Ac] sophorose moiety. Hence, using Equations. (1,2), and (3) (above) and experimentally

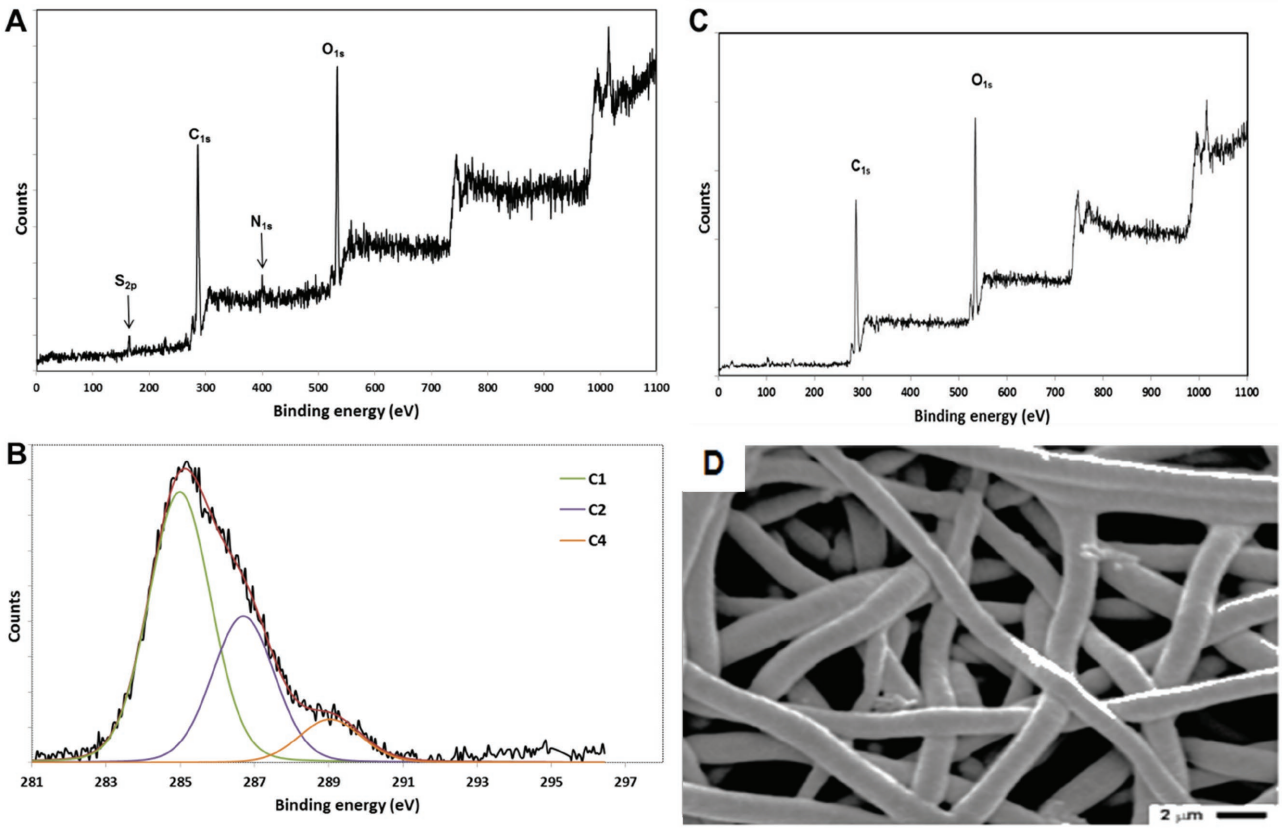

Figure 7. A) XPS spectrum (t.o.a 45°) widescan of aminated polyLSL[6′Ac,6″Ac] mat, B) C_{1s} envelope and its components of aminated polyLSL[6′Ac,6″Ac] mat, C) XPS spectrum (t.o.a 45°) widescan of polyLSL[6′Ac,6″Ac] mat treated with cysteamine and sodium cyanoborohydride but not subjected to the oxidation step, and D) SEM micrograph of aminated polyLSL[6′Ac,6″Ac] mat.

Table 3. Experimental atomic ratios and calculated number of cysteamine molecules per repeat unit of aminated polyLSL[6′Ac,6″Ac] fiber mats.

t.o.a.	Experimental atomic ratio						Calculated[a)]			
	O/C	N/C	S/C	N/O	N/S	S/O	Eq.(1)	Eq.(2)	Eq.(3)	Average
45°	0.36	0.036	0.036	0.090	1.00	0.090	0.94	1.30	1.15	1.13
80°	0.34	0.033	0.034	0.090	0.95	0.095	1.54	1.19	1.15	1.29

[a)]number of cysteamines per polyLSL[6′Ac,6″Ac] repeat unit calculated from experimentally determined atomic ratios using Equations (1–3).

determined O/C, N/C, and N/O atomic ratios, the following average number of cysteamine moieties per polyLSL[6′Ac,6″Ac] repeat unit was introduced: 1.13 for t.o.a. 45° and 1.29 for t.o.a. 80°. Since an average of two aldehyde groups was introduced per two repeating units, it follows that all adehydic functionalities reacted with cysteamine. The morphology of mat fibers after the reductive amination reactions were analyzed by SEM and no appreciable damage was observed (Figure 7D). In order to exclude that the chemical changes observed by XPS are not due to physically absorbed cysteamine, polyLSL[6′Ac,6″Ac] fiber mats that had not been subjected to the oxidation step were treated with cysteamine and sodium cyanoborohydride under the identical reaction conditions used for reductive amination reactions. The XPS spectra of the obtained samples revealed only negligible traces of sulphur and nitrogen (Figure 7C). This confirms that physical adsorption of cysteamine was not the cause of chemical changes determined by XPS.

The last step of fiber mat modification was to perform thiol-ene chemistry, catalyzed by UV irradiation in the presence of a photoinitiator (DMPA), to conjugate the thiol groups of fiber mats to 4-pentenoyl moieties appended to the N-terminus of oligo(Glu_{70}-*co*-Leu_{30}) peptides (Scheme 1). In parallel, this reaction was repeated under identical experimental conditions except without UV irradiation. In both cases, the XPS widescan surface analysis reveals the presence of sulfur, carbon, nitrogen, and oxygen and the respective experimental atomic ratios are listed in Table 4. Calculated atomic ratios are also reported in Table 4, based on the hypothesis that all thiol groups react with terminal alkene moieties of N-(4-pentenoyl)oligo(Glu_{70}-*co*-Leu_{30}).

Table 4. Experimental atomic ratios determined by XPS of polyLSL[6′Ac,6″Ac] fiber mats functionalized with N-(4-pentenoyl) oligo(Glu_{70}-*co*-Leu_{30}) by the thiol-ene "click" reaction with and without UV irradiation. Calculated atomic ratios also reported.

	UV		Without UV		Calculated
t.o.a.	45°	80°	45°	80°	–
O/C	0.34	0.32	0.32	0.34	0.41
N/C	0.10	0.10	0.073	0.070	0.13
S/C	0.014	0.014	0.029	0.028	0.0081
N/O	0.30	0.33	0.20	0.19	0.32
N/S	7.41	7.48	2.47	2.44	16.2
S/O	0.041	0.044	0.080	0.077	0.020

To determine polyLSL[6′Ac,6″Ac] surface functionalization with oligo(Glu_{70}-*co*-Leu_{30}), the N/S ratio was evaluated. If all SH groups (i.e., one per residue on average) are converted to peptide, the N/S ratio should be 16 (Table 4). By contrast, if the click reaction does not take place, the N/S ratio will be unchanged (equal to 1). The experimental N/S ratio of 7.4 (Table 4) shows that nearly 1 out of 2 SH groups undergoes the thiol-ene reaction with alkene terminated peptide. Consequently, about 50 mol% of polyLSL[6′Ac,6″Ac] repeat units at fiber surfaces are decorated with a peptide moiety. In the absence of UV irradiation, the experimental N/S value is 2.4 instead of 1, which would be expected if no reaction or peptide physical adsorption occurs. This suggests that, in the presence of UV irradiation, about 1/3 of the oligo(Glu_{70}-*co*-Leu_{30}) units revealed by XPS are physically adsorbed to polyLSL[6′Ac,6″Ac].

In addition to the above, the C_{1s} envelope profile for peptide decorated polyLSL[6′Ac,6″Ac] was analyzed (Figure 8A). The characteristic signal of aliphatic amide was clearly observed as a shoulder in the C_{1s} envelope (pale blue) centered at 288 eV.[45] By contrast, deconvolution of the C_{1s} envelope of the control (without UV irradiation) shows a much less prominent band centered at 288 eV that is associated with physically adsorbed peptide discussed above (Figure 8B).

4. Conclusions

This paper describes the successful electrospinning of poly(sophorolipid), polyLSL[6′Ac,6″Ac], into fibers that were surface modified with a model peptide. PolyLSL[6′Ac,6″Ac] was selected for this work due to its: (i) promising biocompatibility, (ii) ability to bioresorb at times that are regulated by the hydrophobicity of groups appended to sophorose units, and (iii) the availability of LSL in large

Macromolecular Journals

Macromol. Biosci. **2016**, DOI: 10.1002/mabi.201600327

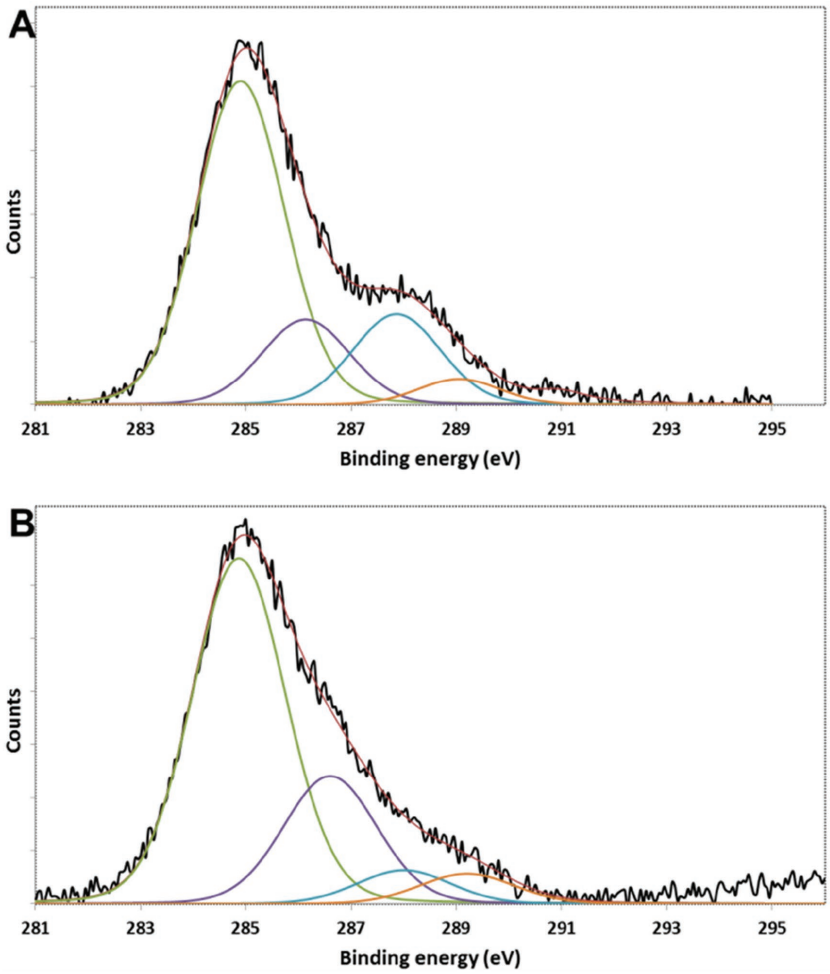

Figure 8. XPS C_{1s} envelope deconvolution of products from reaction of thiol functionalized polyLSL[6′Ac,6″Ac] mats with 4-pentenoyl functionalized oligo(Glu_{70}-*co*-Leu_{30}): A) with and B) without UV irradiation.

quantities based on its efficient production by yeast fermentations. The electrospinning of polyLSL[6′Ac,6″Ac] was successfully performed giving randomly oriented and beadless fibers that are circular in shape (diameter of 1.19 ± 0.16 μm). Analysis of the mat mechanical properties showed that it has an elastic modulus and strain at break of 112 ± 6 Mpa and 206 ± 22%, respectively. Subsequently, work was performed to develop a reliable, facile, and versatile synthetic strategy that can ultimately be used to conjugate peptides with desired biological properties onto precisely engineered electrospun polyLSL fiber mats. For this model study we used the peptide oligo(γ-L-Glu_{70}-*co*-L-Leu_{30}), synthesized by protease catalysis such that it has on average seven repeat units. The N-terminus of oligo(γ-L-Glu_{70}-*co*-L-Leu_{30}) was functionalized with an alkene terminal group. XPS was used to characterize the surface chemical composition of synthesized and modified polyLSL[6′Ac,6″Ac] fiber mats. Fiber modification involved the following steps: (i) periodate oxidation of sophorose moieties such that 2,3-diols of glucose rings were converted to dialdehydes, (ii) reductive amination of dialdehydes with cysteamine and sodium cyanoborohydride to introduce thiols, and (iii) thiol-ene coupling of peptide N-terminal alkenes to the thiol groups on fiber surfaces. XPS was used to analyze the results of each step for the surface functionalization reactions. The results showed that: (i) an average of two aldehyde groups were introduced per two repeating units, (ii) all aldehyde functionalities reacted with cystamine, which has a terminal thiol moiety, and (iii) about 50 mol% of polyLSL[6′Ac,6″Ac] repeat units at fiber surfaces were decorated with the peptide, out of which about 1/3 of the oligo(Glu_{70}-*co*-Leu_{30}) units revealed by XPS are physically adsorbed to polyLSL[6′Ac,6″Ac]. The obtained glycopolymer electrospun materials, conjugated with biomolecules, are expected to have high potential as biomimetic and bioactive tissue scaffolds in tissue engineering and controlled drug delivery applications.

Acknowledgements: The authors are grateful for the funding received from the National Science Foundation Division of Materials Research under the Biomaterials (BMAT) Program (Award 15084222) and from MIUR (Italian Ministry of Education, University and Research).

Received: August 1, 2016; Revised: September 14, 2016; Published online: ; DOI: 10.1002/mabi.201600327

Keywords: electrospinning; fiber mats; oligopeptide; poly(sophorolipid); XPS analysis

[1] F. Rossi, M. van Griensven, *Tissue Eng.* **2014**, *20*, 2043.
[2] E. S. Place, N. D. Evans, M. M. Stevens, *Nat. Mater.* **2009**, *8*, 457.
[3] M. Hashida, M. Hirabayasha, Y. Takakura, *J. Control. Release* **1997**, *46*, 129.
[4] J. Sedó, J. Saiz-Poseu, F. Busqué, D. Ruiz-Molina, *Adv. Mater.* **2013**, *25*, 653.
[5] M. N. Collins, C. Birkinshaw, *Carbohydrate Polym.* **2013**, *92*, 1262.
[6] V. D. Prajapati, G. K. Jani, S. M. Khanda, *Carbohydrate Polym.* **2013**, *95*, 540.
[7] M. Balamurugan, *Int. J. Pharm. Pharm. Sci.* **2012**, *4*, 54.
[8] X. Liu, J. M. Holzwarth, P. X. Ma, *Macromol. Biosci.* **2012**, *12*, 911.

[9] H. Tian, Z. Tang, X. Zhuang, X. Chen, X. Jing, *Prog. Polym. Sci.* **2012**, *37*, 237.
[10] R. Riva, S. Schmeits, F. Stoffelbach, C. Jerome, R. Jerome, P. Lecomte, *Chem. Commun.* **2005**, *42*, 5334.
[11] B. Parrish, R. B. Breitenkamp, T. Emrick, *J. Am. Chem. Soc.* **2005**, *127*, 7404.
[12] M. Leemhuis, N. Akeroyd, J. A. W. Kruijtzer, C. F. van Nostrum, W. E. Hennink, *Eur. Polym. J.* **2008**, *44*, 308.
[13] A. H. Ghassemi, M. J. van Steenbergen, H. Talsma, C. F. van Nostrum, W. Jiskoot, D. J. A. Crommelin, W. E. Hennink, *J. Control. Release* **2009**, *138*, 57.
[14] R. Kumar, W. Gao, R. A. Gross, *Macromolecules* **2002**, *35*, 6835.
[15] X. Chen, R. Gross, *Macromolecules* **1999**, *32*, 308.
[16] C. B. Cooley, B. M. Trantow, F. Nederberg, M. K. Kiesewetter, J. L. Hedrick, R. M. Waymouth, P. A. Wender, *J. Am. Chem. Soc.* **2009**, *131*, 16401.
[17] R. Narain, *Engineered Carbohydrate-Based Materials for Biomedical Applications: Polymers, Surfaces, Denrimers, Nanoparticles, and Hydrogels*, Wiley, Hoboken, NJ, USA **2011**.
[18] M. Ahmed, P. Wattanaarsakit, R. Narain, *Eur. Polym. J.* **2013**, *49*, 3010.
[19] L. Zhang, J. Bernard, T. P. Davis, C. Barner-Kowollik, M. H. Stenzel, *Macromol. Rapid Commun.* **2008**, *29*, 123.
[20] N. Xiao, H. Liang, J. Lu, *Soft Matter* **2011**, *7*, 10834.
[21] J. M. Fishman, L. L. Kiessling, *Angew. Chem. Int. Ed.* **2013**, *52*, 5061.
[22] P. A. Gorin, J. F. T. Spencer, A. P. Tulloch, *Can. J. Chem.* **1961**, *39*, 846.
[23] I. Van Bogaert, K. Saerens, C. D. Muynck, D. Develter, U. Soetaert, E. J. Vandamme, *Appl. Microbiol. Biotechnol.* **2007**, *76*, 23.
[24] P. A. Felse, V. Shah, J. Chan, K. J. Rao, R. A. Gross, *Enzyme Microb. Technol.* **2007**, *40*, 316.
[25] K. Bisht, W. Gao, R. A. Gross, *Macromolecules* **2000**, *33*, 6208.
[26] Y. Hu, L. K. Ju, *Biotechnol. Progress* **2003**, *19*, 303.
[27] W. Gao, R. Hagver, V. Shah, W. Xie, R. A. Gross, M. F. Ilker, C. Bell, K. A. Burke, E. B. Coughlin, *Macromolecules* **2007**, *40*, 145.
[28] Y. Peng, J. Decatur, M. A. R. Meier, R. A. Gross, *Macromolecules* **2013**, *46*, 3293.
[29] E. Zini, M. Gazzano, M. Scandola, S. R. Wallner, R. A. Gross, *Macromolecules* **2008**, *41*, 7463.
[30] K. Bisht, R. A. Gross, D. Kaplan, *J. Org. Chem.* **1999**, *64*, 780.
[31] Y. Peng, D. J. Munoz-Pinto, M. Chen, J. Decatur, M. Hahn, R. A. Gross, *Biomacromolecules* **2014**, *15*, 4214.
[32] S. Agarwal, J. H. Wendorff, A. Greiner, *Polymer* **2008**, *49*, 5603.
[33] D. Liang, B. S. Hsiao, B. Chu, *Adv. Drug Deliv. Rev.* **2007**, *59*, 1392.
[34] T. J. Still, H. A. von Recum, *Biomaterials* **2008**, *29*, 1989.
[35] H. S. Yoo, T. G. Kim, T. G. Park, *Adv. Drug Deliv. Rev.* **2009**, *61*, 1033.
[36] V. Guilmanov, A. Ballistreri, G. Impallomeni, R. A. Gross, *Biotechnol. Bioeng.* **2002**, *77*, 489.
[37] G. Li, V. K. Raman, W. Xie, R. A. Gross, *Macromolecules* **2008**, *41*, 7003.
[38] M. Bertoldo, G. Zampano, F. La Terra, V. Villari, V. Castelvetro, *Biomacromolecules* **2011**, *12*, 388.
[39] K. A. Kristiansen, A. Potthast, B. E. Christensen, *Carbohydrate Res.* **2010**, *345*, 1264.
[40] R. P. Tripathi, S. S. Verma, J. Pandey, V. K. Tiwarib, *Curr. Org. Chem.* **2008**, *12*, 1093.
[41] K. L. Killops, L. M. Campos, C. J. Hawker, *J. Am. Chem. Soc.* **2008**, *130*, 5062.
[42] D. T. Clark, H. R. Thomas, *J. Polym. Sci., Polym. Chem. Ed.* **1977**, *15*, 2843.
[43] M. S. Rizvi, P. Kumar, D. S. Katti, A. Pal, *Acta Biomater.* **2012**, *8*, 4111.
[44] D. Briggs, M. P. Seah, *Practical Surface Analysis*, 2nd ed., Wiley, New York **1990**, Vol. *1*, p. 437.
[45] G. Beamson, D. Briggs, *High Resolution XPS of Organic Polymers: The Scienta ESCA300 Database*, Wiley, Chichester **1992**.

Macromol. Biosci. **2016**, DOI: 10.1002/mabi.201600327